Tribology International 53 (2012) 179–184

Contents lists available at SciVerse ScienceDirect

Tribology International

journal homepage: www.elsevier.com/locate/triboint

Short Communication

Mechanism of material removal during tribological behaviour of aluminium matrix (Al–Zn–Mg–Cu) composites

R.N. Rao [a,*], S. Das [b], D.P. Mondal [b], G. Dixit [c]

[a] Department of Mechanical Engineering, National Institute of Technology (NITW), Warangal 506 021, AP, India
[b] Advanced Materials and Processes Research Institute (AMPRI), Bhopal 462 026, India
[c] Maulana Azad National Institute of Technology (MANIT), Bhopal 462 007, India

ARTICLE INFO

Article history:
Received 27 December 2011
Received in revised form
14 April 2012
Accepted 17 April 2012
Available online 27 April 2012

Keywords:
Al–Zn–Mg–Cu alloy
Sliding wear
MML
Wear mechanism.

ABSTRACT

In the present study an attempt is made to synthesise Al–Zn–Mg–Cu alloy–SiC particle reinforced composite using liquid metallurgy route and to characterize the composites in terms of microstructure and sliding wear. It is to be noted that seizure pressure is enhanced by 37.5% due to the addition of 10 wt% of SiC particles in aluminium alloy. The wear mechanism is dictated by the formation and stability of oxide layer, mechanically mixed layer (MML) and subsurface deformation and cracking. There is also mutual transfer of pin surface and counter surface materials. The critical load at which MML gets removed is also examined. These phenomenon are represented schematically in this paper and the wear mechanism is explained.

1. Introduction

Aluminium matrix composites (AMCs), reinforced with hard ceramic particles, have emerged as potential materials especially for wear resistant and weight critical applications [1–4]. In general, AMCs offer superior wear and seizure resistance as compared to the alloy irrespective of applied load and sliding speed. This is primarily due to the fact that the hard dispersoid makes the matrix alloy plastically constrained and improves the strength of the matrix alloy [5,6]. Additionally, the hard dispersoids present on the surface of the composite as protrusions and protects the matrix from the severe contact with the counter surfaces [7,8] and thus, resulting in less wear, lower coefficient of friction and temperature rise, in composite, as compared to that in the alloy [9]. Wilson and Alpas [10] presented wear mechanism maps for A356 alloy–SiC composites, in which four wear regimes were observed in the composites and the alloy depending on speed and applied load. These regions are mild wear, oxidative wear, delamination wear and severe wear. Mild wear occurs usually at very slow speed and lower applied load. At relatively slower speed, if the load increases considerably, mixing of wear debris and counter face material could take place which due to higher temperature, gets oxidised and termed as oxidative wear. The oxidised layer may cover the surface and reduce the wear rate. The formation and removal of this layer determines the overall wear rate of the material. At higher load, this layer is easily broken and removed from the specimen surface and thus resulting higher wear rate with applied load and sliding speed. At higher sliding speed, and relatively lower applied load, wear by delamination mechanism is prevailing. This may be due to more adiabatic type of heating and cause more adhesive action between the two surfaces. Severe subsurface cracking could take place due to the shear type of deformation of the mixed layer and plastic incompatibility between mixed layer and the underlying material. The subsurface deformation (which may be the important factor for subsurface cracking) and subsurface microstructural changes have been reported by many investigators [11,12]. Severe subsurface cracking leads to delamination of mixed layer from the wear surface. At a critical applied load and sliding velocity, temperature rises so high and because of severe degree of delaminaiton, mixed layer become discontinuous and naked material come in contact with counter surface. This also leads to rise in surface temperature to a critical value, i.e., flashing temperature at which strong adhesion between counter surface and specimen took place [13]. This leads to severe wear and on-set of seizure. The wear mechanism map also demonstrates that the seizure temperature of A356 alloys is 125 °C and it is increased significantly by addition of 20% SiC to 378 °C. The critical load and sliding speed for seizure are interdependent. At slower speed, higher load may lead to seizure of the material. Improvement in wear and seizure resistance due to addition of SiC particles may be attributed to reduction in propensity of material flow at the surface and more thermally stable mixed layer formed [4]. Alpas and Zhang [14] schematically showed how the SiC particles help in forming a mixed layer on the contact surface of

* Corresponding author. Tel.: +91 9441569066; fax: +91 8702459547.
E-mail address: rnraonitw@gmail.com (R.N. Rao).

0301-679X/$ - see front matter © 2012 Elsevier Ltd. All rights reserved.
http://dx.doi.org/10.1016/j.triboint.2012.04.017

composite specimen. The mixed layer consists of base alloy, oxides of base alloy and counter surface, counter surface material and fragmented ceramic reinforcement [15,16]. The presence of iron and iron oxide has been confirmed by several investigators through X-ray diffraction [10,13] study or energy dispersive X-ray (EDX) analysis [10,17]. Subsurface deformation (shear type) which causes fragmentation of fibres/whiskers followed by mixing in the interface layer has been clearly demonstrated by few investigators [10,18,19]. The fracturing tendency of the fibre is reported to be more than that of whisker [20]. The probability of fracture of particle increases with increase in particle size. Greater degree of fracture of particles or fibre leads to more brittle MML which is easily detached from wear surface or coarser particle itself abrade the MML leading to higher wear rate. It is also reported that the counter surface material is also transferred into the mixed layer and more transfer of material could be taken place in case of composite. The transfer of counter surface material increases with increase in reinforcement content [5,10,13].

2. Experimental

Aluminium matrix composite was synthesised through solidification processing (stir-casting) route using AA7010 alloy (Al–Zn–Mg–Cu) as matrix and SiC particle (size range: 20–40 μm, wt% 10) composites have been used for the present study. The alloy having chemical composition of Fe – 0.27%, Cu – 1.28%, Mg – 1.14%, Zn – 5.30%, Al – rest. The composite and the alloy were cast in the form of cylinders of dimension: 200 mm in length and 16 mm in diameter, in a permanent cast iron die. The cast samples were mechanically polished and etched with Keller's reagent (1% HF, 1.5% HCl, 2.5% HNO_3 and remaining water) for microstructural study using SEM (model: JEOL, JSM-5600). The etched samples were sputtered with gold prior to SEM examination.

The alloy and composites were heattreated in a Muffle electric furnace. Three stages involved during heat treatment of the investigated material are: (i) Solution treatment: the alloy or composite are heated for 8 h at a temperature of 490 °C until the alloying solute elements are completely dissolved in Al solid solution; (ii) quenching: the solution treated material is cooled rapidly in the water to prevent the precipitation of the solute elements and to obtain a super saturated solid solution; and (iii) artificial aging: hardening can be done by reheating the quenched alloy to a temperature of 180 °C for 4, 6, 8 and 10 h in order to get the better properties.

Sliding wear tests were conducted in dry condition using pin-on-disc wear testing apparatus (model: TR20-LE, Wear and Friction Monitor, Ducom Make, Bangalore, India) against EN32 steel disc having hardness of 470Hv. The pin-samples were machined from the cast cylinders of dimensions 27 mm in length and 8 mm in diameter. The samples were tested at different applied pressures and the sliding distances were varied up to 5000 m. The wear rate was measured from the weight loss measurement and is expressed in terms of m^3/m. The fresh sample was used for each test and is allowed to travel desired distance. The maximum load selected in the present study is the load at which the sample gets seized, i.e., the seizure pressure. The temperature rise and frictional forces were recorded from the digital display. A thermocouple was inserted into a small drill made on the specimen near to the contacting surface (2 mm from the contact surface) for measuring the temperature.

3. Results and discussion

Fig. 1(a) shows the microstructure of AA7010-10% SiC composite showing uniform distribution of SiC particle in Al alloy matrix. Higher magnification micrograph of composite clearly shows good bonding between particle and the matrix (Fig. 1(b)). Fig. 2 shows that the seizure pressure of the alloy and composite in cast and heat treated conditions. It noted that seizure pressure is enhanced by 37.5% due to the addition of 10 wt% of SiC particles in aluminium alloy, in as cast sample. The heat treated alloy shows 12.5% improvement in seizure pressure as compared to cast alloy. However, the improvement in the seizure pressure of the composite due to heat treatment is around 50% as compared to cast alloy. It is noted that heat treatment leads to considerable improvement in the transition load or seizure pressure in the alloy samples as well as in the composite. The seizure pressure of the composite is noted to be considerably higher than that of the alloy. It is evident from Fig. 3 of the bar chart that the wear rate in all the samples decreases due to the addition of SiC content and heatreattratmet irrespective of the material. Fig. 4 shows the recorded temperature at various materials during sliding wear. It is noted that temperature rise is more in the case of composite as compared to alloy irrespective of the surface conditions. It is further noted from Fig. 4 that initially the temperature increases slowly with applied pressure and after a certain pressure it increased very rapidly. It is understood that rapid increase in temperature is primarily due to on set of seizure. The composite seizes at a temperature of 166 °C and 164 °C for heat treated and as cast conditions respectively. The alloy, on the other hand, seizes at a temperature of 158 °C and 152 °C in as cast surface and heat treated condition respectively. It is inferred from the above results that the thermal stability of alloy is enhanced by reinforcing SiC particle and heat treatment. Fig. 5 represents coefficient of friction for alloy and composite in as cast and heat treated condition, there is no definite trend for comparison of coefficient of friction between alloy and composite. In lower applied pressure alloy exhibits higher value of coefficient of friction, whereas at

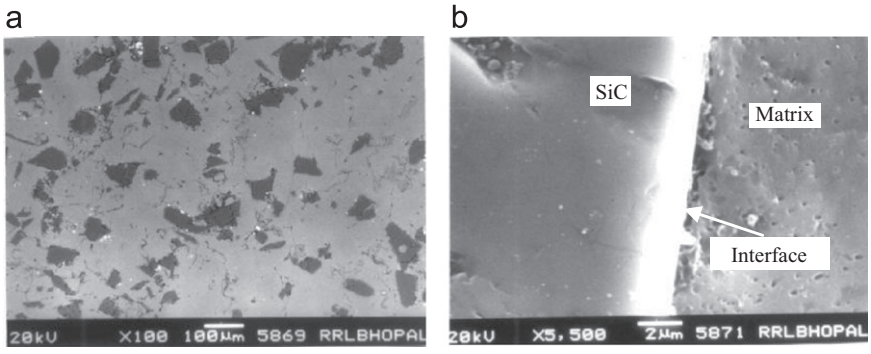

Fig. 1. Microstructure of alloy and composite: (a) alloy showing aluminium dendrites and intermetallic precipitates, (b) distribution of particles in composite and (c) interface between particle and matrix.

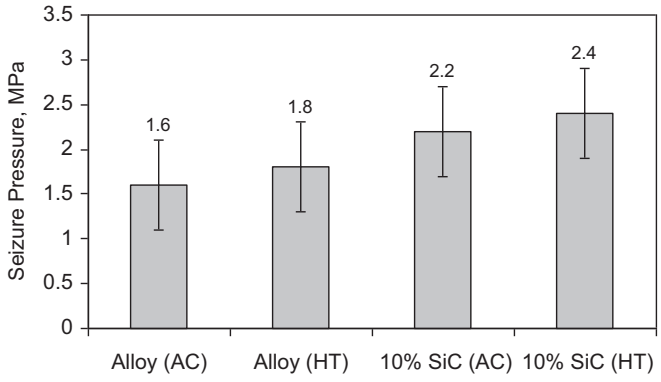

Fig. 2. Seizure pressure of the material.

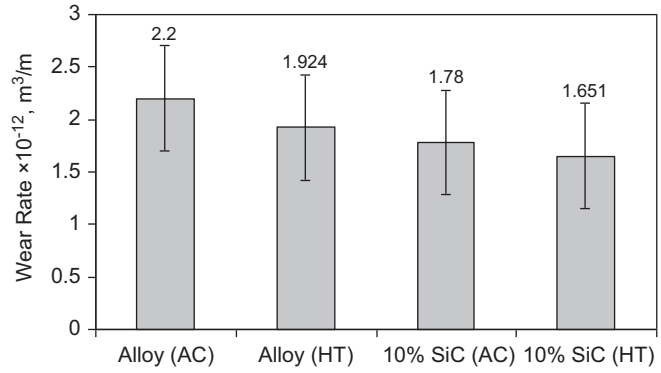

Fig. 3. Wear rate of the material.

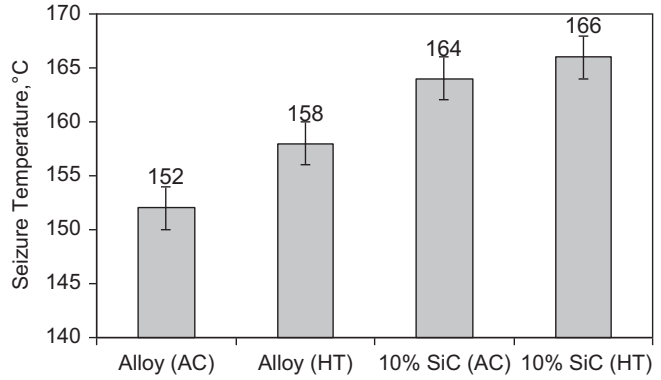

Fig. 4. Seizure temperature of the material.

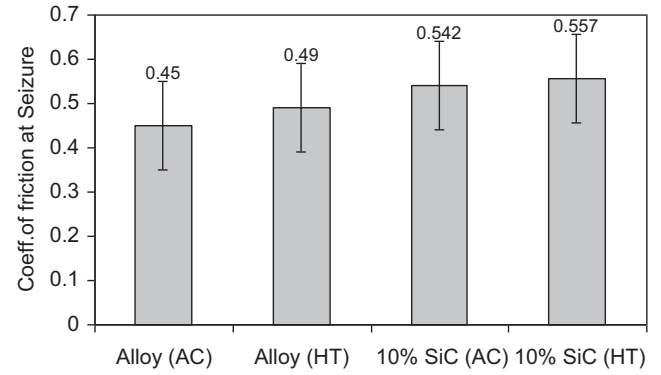

Fig. 5. Coefficient of friction at the seizure of the material.

higher pressure the reverse is true. But in the present study there is no much difference is observed irrespective of the material.

The mechanism of material removal in case of alloy and composite is schematically represented in Figs. 6 and 7, respectively. Stage (I) (Fig. 6) shows the asperity-to-asperity contact in the initial period of sliding wear of the alloy. Some of the asperities make contact at the tip. The asperities of counter surface having grater height penetrate deep into the softer surface. Further, some of the asperities of counter surface and specimen surface make contact along their sidewalls. Stage (II) (Fig. 6) shows initiation of plastic deformation at the surface and subsurface and leading to alignment of particles towards sliding direction and plastic deformation at the asperity-to-asperity contact. It also shows generation of grooves due to scratching action of asperities on the counter surface and formation of wear debris due to fracture of few asperities. Stage (III) (Fig. 6) depicts compaction of wear debris on the specimen surface forming mechanically mixed layer and significant amount of subsurface

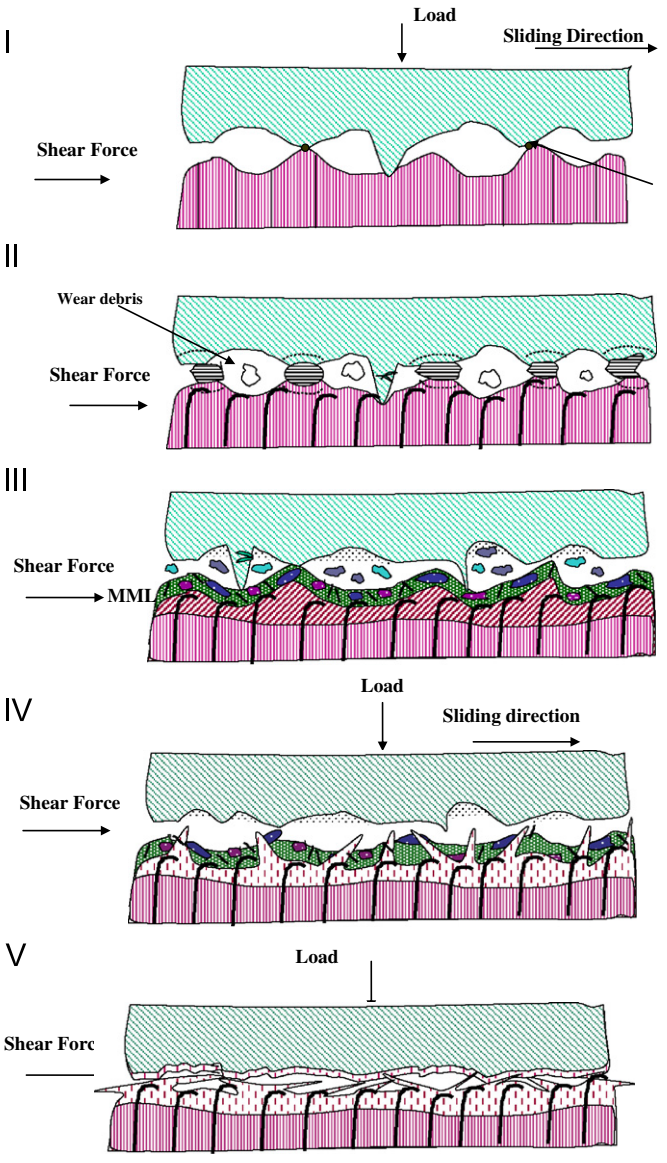

Fig. 6. Wear mechanism of alloy. Stage I. (Fig. 6): Asperity to asperity contact, Stage II. (Fig. 6): Asperity deformation, Fracture, Stage III (Fig. 6): Formation of MML/mixed oxide layer and subsurface deformation, Stage IV (Fig. 6): Fracture of MML/MOL and partially melting of subsurface and delamination of MML/MOL and Stage V (Fig. 6): Adhesion between the counter surfaces.

Fig. 7. Wear mechanism of composite. Stage I (Fig. 7): Protruded SiCp penetrate in to the counter face, Stage II (Fig. 7): Micro grooving on the counter surface (formation of wear debris, fracture of sharp asperities interaction of these wear debris to O_2), Stage III (Fig. 7): Micro cracking of protruded SiC particles (plastically deformed), Stage IV (Fig. 7): Compact of wear debris (eqiaxed and elongated) and forming MML and partially oxidized, Stage V (Fig. 7): Counter surface become smoother, accommodated, some amount of material transferred from the composite surface, Stage VI(Fig. 7) : Fragmentation of elongated wear debris in MML and cracking of MML, Stage VII (Fig. 7) : Partial melting of plastically deformed subsurface of composite and Stage VIII (Fig. 7): Adhesion between the counter surfaces (seizing of the composite).

deformation leading to alignment of precipitates and other micro-constituents towards sliding direction. Stage (IV) (Fig. 6) shows partial melting of subsurface region (onset of seizure), which comes out through the crack of the MML and exposed to the counter surface. The valleys of asperities of counter surface get accommodated by the material transferred from specimen surface. Stage (V) (Fig. 6) represents that the MML gets removed from the specimen surface and partially melted subsurface material flows over the worn surface and gets adhered to counter surface leading to seizure. Because of the flow of partially melted specimen surface, the worn surface in seizure looks like wave like flow of material on the specimen surface after seizure.

Fig. 7 shows the schematic diagram indicating mechanism of material removal of Al–SiC composites during sliding wear. Stage (I) (Fig. 7 represents the contact between counter surface and composite surface, which are in relative motion against each other under normal applied load. It shows contact between the asperities of counter surface and the matrix of composite material, penetration of longer asperities of counter surface to the matrix of composite material and protruded SiC particles which penetrate into the counter surface. Stage (II) represents formation of fine wear debris due to fracture of sharp asperities. Stage (III) (Fig. 7) shows micro cracking of protruded SiC particles, formation of large number of elongated and equiaxed wear debris which are getting accommodated on the contact surfaces. In addition the subsurface region gets plastically deformed. Stage (IV) (Fig. 7) represents that the wear debris at the contact surfaces gets compacted and going to form mechanically mixed layer over the composite surface as well as transfer of some material to the counter surface. The MML in composite is the mixture of partially oxidised, equiaxed and elongated wear debris generated from matrix of composite material and counter surface material along with fine SiC particle. Stage (V) (Fig. 7) shows that the counter surface become smoother and accommodated some amount of material transferred from the composite surface. As the counter surface comes in contact with MML the transferred material is expected to be similar to the MML. This stage also shows that the MML is discontinuous along the area containing SiC particle. Stage (VI) (Fig. 7) demonstrates that fragmentation of elongated wear debris in MML and cracking of the MML along the interface of the compacted wear debrises. Stage (VII) of Fig. 6 represents that partial melting of plastically deformed subsurface just below MML and flow of partially melted subsurface through the wide cracks generated in MML. The cracking of MML is facilitating due to upward thrust given by the flow of the partially melted sub-layer and the plastic and thermal incompatibility between MML and sub-layer. The fragmented MML in due course gets delaminated from the wear surface and the partially melted sub layers comes in direct contact with counter surface. Stage (VIII) (Fig. 7) shows the flow of partially melted sub layer which comes through the crack in MML and thus forming wave like flow of partially melted material on the composite surface which subsequently gets adhered to the counter surface. This stage referred to the seizing of the composite surface. This stage also shows that the flow of partially melted sub layer is resisted by the presence of SiC particle, which in other words leads to particles, which penetrate into the counter surface.

Fig. 8 shows the worn surface of (a) alloy at higher applied pressure shows severely damaged surface and formation of longitudinal and transverse cracks (marked 'A'), relatively smoother MML/MOL (marked 'B') it also shows debris about to fall off from the wear surface(arrow marked) and (b) composite, at lower sliding speed and lower applied pressure, continuous grooves (marked 'A'), MML/MOL (marked 'D'), exposed SiC particles (marked 'B') patches of damaged regions (marked 'C') and also pitting marks (arrow marked) on the wear surface marks and badly damaged (marked A) in some places.

Comparison of the schematic representation of sliding wear of alloy and composite against steel counter surface clearly demonstrates that the transfer of counter surface materials to the MML is more in case of composite as compared to the alloy and the extent of transfer of counter surface materials increases with increase in applied pressure. The MML or the subsurface layer of composite has higher strength and hardness as compared to the alloy. Which make it suitable to withstand more pressure and temperature. In near to the seizure pressure, the MML becomes unstable and get delaminated readily from the specimen surface. At the point of seizure there will be hardly any trace of MML on specimen surface this is exactly experimentally observed from SEM analysis on subsurface and wear surfaces at different loading conditions.

The wear rate as a function of applied pressure in case of sliding wear is expressed by Archard [21] law of wear equation, which states that the wear rate increases linearly with increasing applied pressure. This is primarily due to the fact that with increase in applied pressure, the penetration of hard asperities of the counter surface to the softer pin surface increases and also the deformation and fracture of asperities of the softer surface increases. Again, on the other hand more amount of softer material from the pin surface get accumulated at the valleys between the asperities of counter surface resulting in decrease in asperity height of the counter surface. This leads to reduction in cutting efficiency of counter surface asperities. Again, with increase in applied pressure surface and subsurface deformation and micro cracking tendency increases. The effective wear from the specimen surface is due to the combined effect of all these above mentioned factors. In the present investigation it is also noted that up to certain applied load (before seizure) the wear rate increases more or less linearly with applied pressure. But the rate of increase in wear rate with applied pressure within this range is not so significant. However, when the applied pressure reaches to a critical value the frictional heating becomes significantly high and thus the localised adhesion of the pin surface with the counter surface increases and also because of softening of the surface material the penetration of the asperities increases significantly. Under such conditions the material removal due to delamination of adhered areas, micro cutting and micro fracturing increases significantly. This leads to destruction of MML, which might be forming at lower applied load at the initial period of sliding. As a result, after a critical load there is a transition from

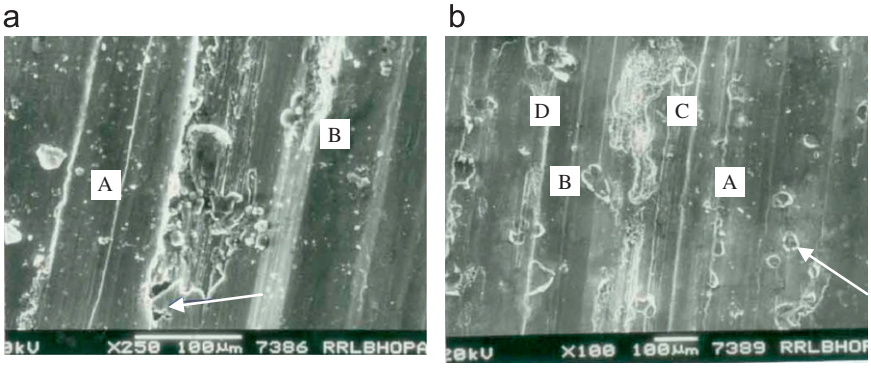

Fig. 8. The wear surface of (a) alloy at higher applied pressure and (b) composite, at lower sliding speed and lower applied pressure.

smooth linear increase wear rate to sudden increase in wear rate. Because of the greater degree of softening of pin surface and considerable higher amount of material transfer between the counter surfaces, the surfaces become smoother. This fact leads to greater degree of sliding action and spreading of softer material on the specimen surface. As a result the wear rate after transition load remains unchanged up to certain applied pressure. But at the point of seizure, the temperature increases significantly, so that the pin surface material gets partially melted and this highly viscous material gets completely adhered with the counter surface and subsequently removed readily from the specimen surface in the form of flash. This leads to sudden increase in wear rate to a significantly higher value, and is identified as seizure of the specimen.

4. Conclusions

1. The sliding wear behaviour of aluminium alloy strongly depends on the surface conditions and the particle reinforcement.
2. Addition of hard particle in the alloy substantially decreases the wear rate and the temperature rise, and increases the seizure pressure. The wear rate increases with increase in applied load.
3. When the samples undergone for heat treatment increase the seizure pressure and seizure temperature and decrease the wear rate, coefficient of friction and temperature-rise irrespective of the material. The improvement is due to the formation of thin oxide coating and formation of smoother surface.
4. However, the improvement in the seizure pressure of the composite due to heat treatment is around 50% as compared to cast alloy.
5. Sliding wear is associated with transfer of counter surface materials and formation and destruction of MML. At lower applied load MML is thinner but stable. At intermediate load MML thickness increases and its iron content increases indicating more stable MML. Above a critical applied load MML become unstable and starts getting destroyed. At seizure load MML is totally destroyed.

References

[1] Nussbaum AI. New applications for aluminium based metal matrix composites. Light Metal Age, 1997:54–8.
[2] Alpas AT, Zhang J. Wear regimes and transitions in Al_2O_3 particulate reinforced aluminum alloys. Material Science and Engineering A 1993;161:273–84.
[3] Mondal DP, Das S, Rao RN, Singh M. Effect of SiC addition and running-in-wear on the sliding wear behaviour of Al–Zn–Mg aluminium alloy. Materials Science and Engineering A 2005;40(1–2):307–19.
[4] Pramila Bai BN, Ramasesh BS, Surappa MK. Dry sliding wear of A356-Al–SiCp composite. Wear, 1992;157:295–304.
[5] Hutchings IM, Wilson S, Alpas AT. Wear of Aluminum-based composites, Comprehensive composite materials, (MMC), 3. Elsevier Science Ltd;; 2000 501–519.
[6] Rao RN, Das S, Mondal DP, Dixit G. Dry sliding wear behaviour of cast high strength aluminium alloy (Al–Zn–Mg) and hard particle composites. Wear, 2009;267:1688–95.
[7] Sannino AP, Rack HJ. Tribological investigator of 2009 Al–20vol% SiCp/17-4 PH, part I: composite performance. Wear 1996;197:151–9.
[8] Sharma SC. The sliding wear behaviour of Al6061–garnet particulate composites. Wear, 2001;249:1036–45.
[9] How HC, Baker TN. Characterization of sliding friction-induced subsurface deformation of Saffil-reinforced AA6061 composites. Wear, 1999;232:106–15.
[10] Wilson S, Alpas AT. Wear mechanism maps for metal matrix composites. Wear 1997;212:41–9.
[11] Ghazali MJ, Rainforth WM, Jones H. The wear of wrought aluminium alloys under dry sliding conditions. Tribology International 2007;40:160–9.
[12] Adel MH, Alrashdan A, Hayajneh MT, Mayyas AT. Wear behavior of Al–Mg–Cu–based composites containing SiC particles. Tribology International 2009;42:1230–8.
[13] Venkataraman B, Sundararajan G. The sliding wear behaviour of Al–SiC particulate composites. II. The characterization of subsurface deformation and correlation with wear beaviour. Acta Metallurgica et Materialia 1996;44:461–73.
[14] Alpas AT, Zhang J. Effect of SiC particulate reinforcement on the dry sliding wear of aluminum–silicon alloys (A356). Wear 1992;155::83–104.
[15] Sahin Y. Tribological behaviour of the metal matrix and its composites. Materials & Design 2007;28:1348–52.
[16] Moore A, Douthwaite RM. Plastic deformation below worn surfaces, Metallurgical. Transactions A, 1976;7:1833–9.
[17] Wang A, Rack HJ. Abraisve wear of silicon carbide particulate and whisker-reinforced 7091 aluminium matrix composites. Wear 1991;146:337–48.
[18] How HC, Baker. TN. Dry sliding wear behaviour of Saffil reinforced AA6061 composites. Wear, 1997;210:263–72.
[19] Cao SQ, Wu JM, Liu Z, Liu G. Wear resistance mechanism of an Al-12Si alloy reinforced with aluminosilicate short fibres, Tribology. International 1999;32:721–4.
[20] Sahin Y. Wear behaviour of aluminium alloy and its composites reinforced by SiC particles using statistical analysis. Materials & Design 2003;24:95–103.
[21] Archard JF. Journal of Applied Physics, 1953;24:981–8.